

Characterization And Control Of The Surface Of MBE-Grown Bi₂Se₃ Topological Insulator Films

Abstract:

As Moore's law is becoming unsustainable with conventional CMOS devices, academic and industrial researchers are looking beyond semiconductor materials for future transistor designs. Topological insulator (TI) materials comprise a class of materials that host helical Dirac fermions at their surfaces, making them promising candidates for spintronic device architectures (Fig. 1). Among the TI class, Bi₂Se₃ has often been cited as the 'prototypical' TI, as it has a relatively simple surface structure (one Dirac cone at the gamma point), and a relatively large band gap (~0.3 eV) that helps maintain an insulating bulk. However, growing Bi₂Se₃ for devices has been problematic. These crystals experience a variety of defects, including inter-QL Bi layers, misoriented grains (often characterizable as a 180° 'twinning' effect), surface roughness, oxidation upon exposure to atmosphere, and Se vacancy formation. These effects tend to result in n-doping, and can often raise the Fermi level to the conduction band, thus effectively removing the surface helicity. **With Professor Chris Hinkle's research group at UT-Dallas, we have begun to study a capping method aimed at eliminating oxidation and doping issues.** The samples were MBE grown on Al₂O₃ substrates, capped with a thick Se layer, and shipped to CNSE in Albany, NY. **This work is aimed at characterizing the Bi₂Se₃ films before and after the Se capped is removed, including tracking the Fermi level after decapping.** We demonstrate that these films are highly crystalline in the bulk and at the surface, that the grain 'twinning' effect has been greatly reduced in these growths, that decapping occurs in one large spike after which the bare Bi₂Se₃ surface is exposed, and that the Fermi level remains within ~40 meV of the Dirac point after decapping. This growth method thus produces high quality Bi₂Se₃, which is suitable for device applications.

Characterization of Se-Capped Bi₂Se₃ Film

Crystallinity-directed characterization methods were employed before thermal decapping in order to assess the quality of MBE Bi₂Se₃ growth, to characterize the Se cap, and to act as a control for any change in Bi₂Se₃ crystallinity caused by the thermal decapping process. As with most materials, conductivity (at the surface, for TIs) is expected to improve with large, well aligned grains. Equally important in TI materials is the improvement of bulk resistivity in large-grain films, due to the minimization of bulk defect states. Further, because 3D TI materials require a sufficiently large, pristine bulk volume to generate a non-trivial electronic topology, extreme polycrystallinity poses a threat to this property, and thus may eliminate topological surface states altogether. While van der Waals bonding in the c-direction of Bi₂Se₃ facilitates flat, vertical QL stacking, Bi bilayers have been observed in between well stacked QLs, and in-plane growth is subject to azimuthal lattice direction variance, even on an ideal hexagonal crystal substrate (Al₂O₃, in this case). This often manifests as 'twinning', a 180° rotation of the 3-fold symmetric lattice between adjacent grains.

Because of their non-destructive tendencies, we employed XRD and SEM to characterize the crystallinity of these films. Vertical stacking order of a sample on a Si carrier wafer is measured with an Omega-2Theta XRD scan (Fig. 4), which shows the following:

- All expected Bi₂Se₃ planes (l=3n) are aligned to each other, as well as to the substrate surface normal (as given by the Al₂O₃ (006) direction). The interface between film and substrate occurs between hexagonal Bi₂Se₃ and Al₂O₃ lattice planes.
- Bi₂Se₃ diffraction plane intensities match theoretical values, with l = 3, 6, and 15 being the most intense. This implies that the film is only composed of stacked QLs, without any Bi bilayers.
- Extra diffraction peaks (other than Bi₂Se₃, Al₂O₃, and Si) were found, and are in good agreement with (h 0 0) Se planes (trigonal, space group 152, α = β = 90°, γ = 120°). This planar orientation does not provide any possible cleavage points for epitaxial growth on the hexagonal (001) surface of Bi₂Se₃.

A high-angle pole figure (tilt ~58° from normal) at the Bi₂Se₃ (015) plane d-spacing was also performed in order to assess the in-plane order. This plane was chosen for its high structure factor (highest in Bi₂Se₃, and for its 3-fold rotational symmetry. Bi₂Se₃ diffraction planes that have l = 3n are 6-fold symmetric, and thus provide no information about twinning. However, for l ≠ 3n, diffraction points are 3-fold symmetric, and give definitive grain orientation information. In the pole figure, six diffraction spots appear, though the 90 ± 120° points are ~40x more intense than the 180 ± 120° points. This indicates that there are two grain domains, with a relative rotation of 180° ('twinning'), but one orientation is dominant. Thus, we can infer that the majority of grains have the (015) plane normal pointing in the same direction, and that twinning is minimized.

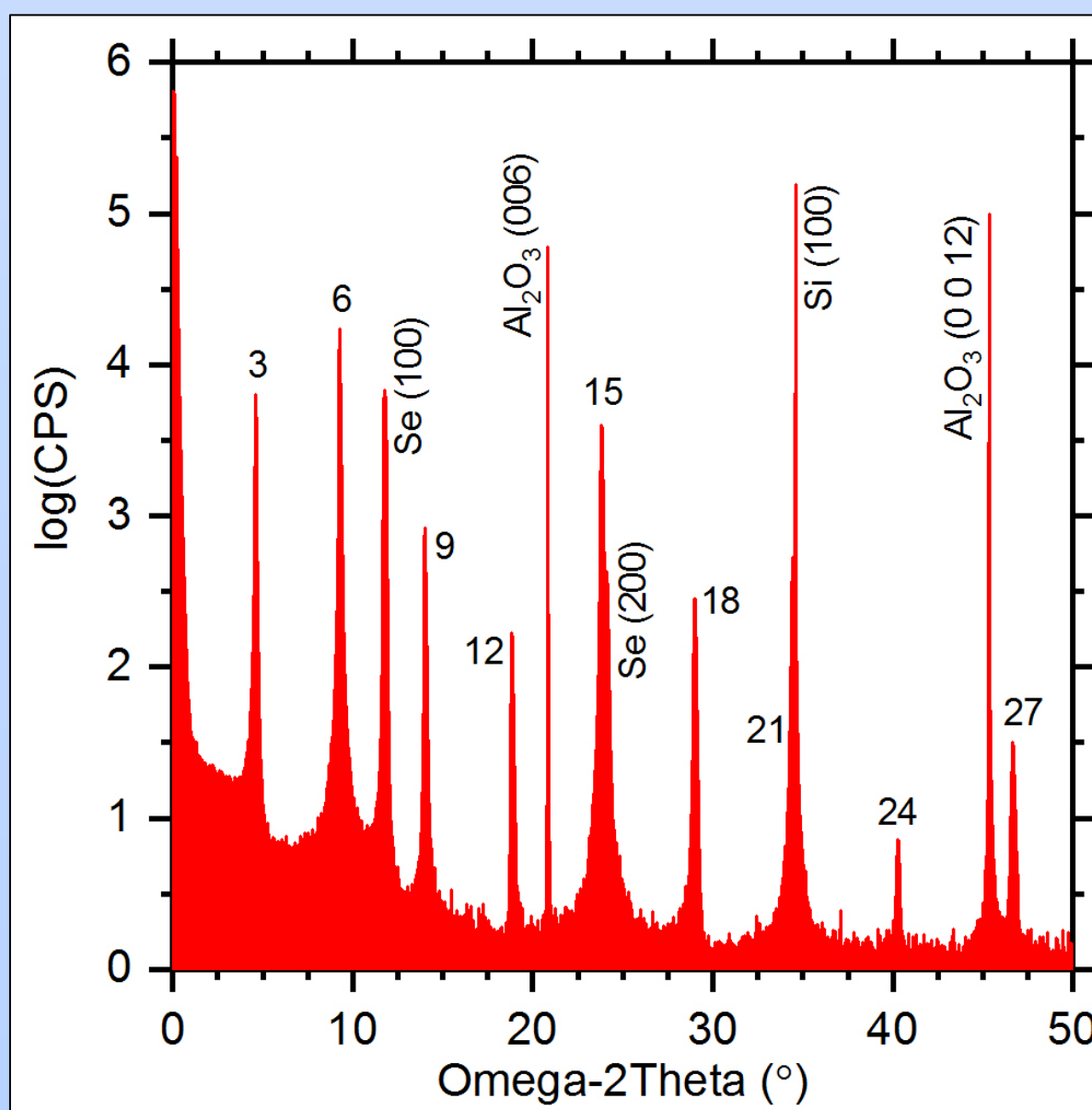


Figure 4: XRD Omega-2Theta scan of Se-capped Bi₂Se₃ sample along surface normal direction. Peaks only marked with numbers indicate the l index of a Bi₂Se₃ diffraction plane, e.g. '3' refers to the (003) plane of Bi₂Se₃. Only (0 0 3n) planes of Bi₂Se₃ are allowed, and they show up with expected intensities. The Se cap was expected to be amorphous, but was found to be crystalline, with the (100) plane aligned to the surface.

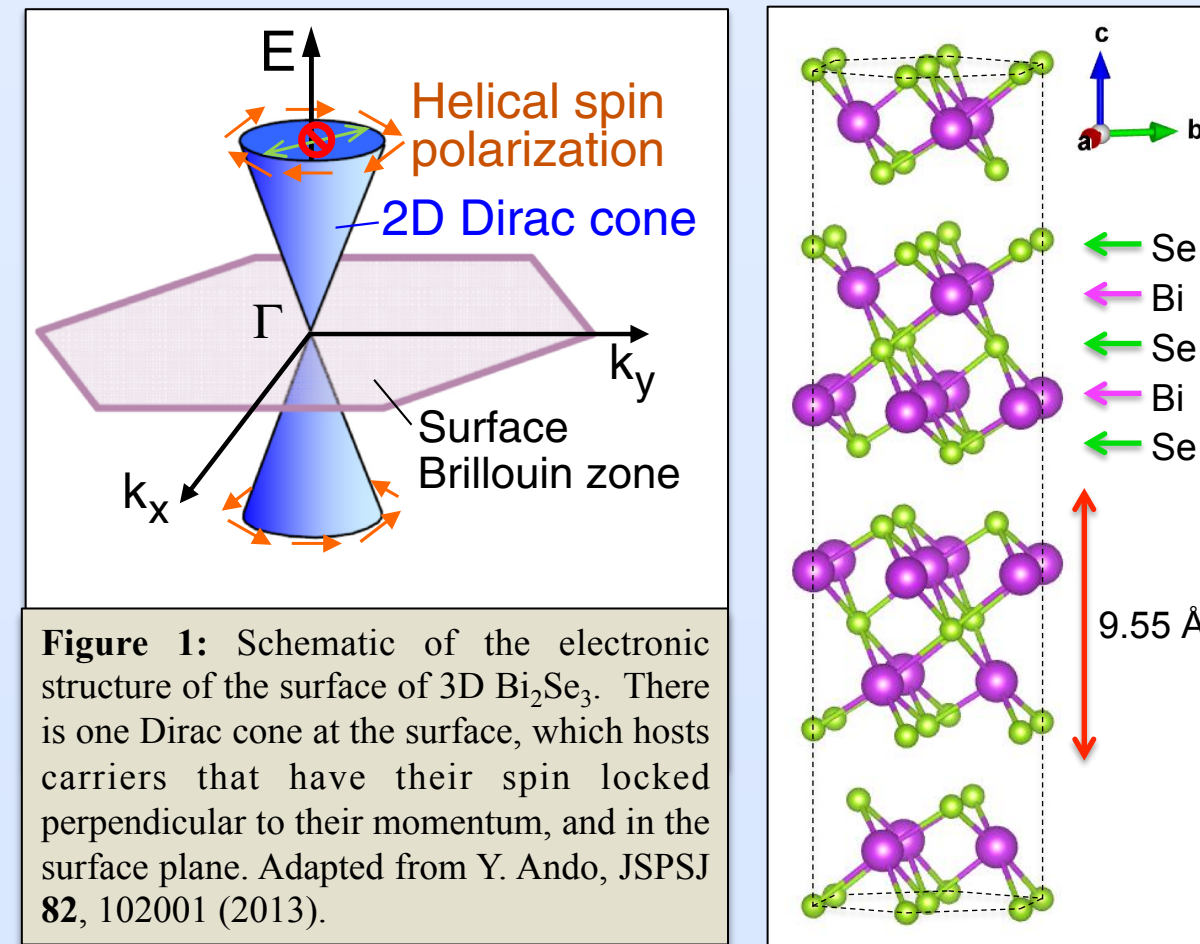


Figure 1: Schematic of the electronic structure of the surface of 3D Bi₂Se₃. There is one Dirac cone at the surface, which hosts carriers that have their spin locked perpendicular to their momentum, and in the surface plane. Adapted from Y. Ando, JPSJ 82, 102001 (2013).

Figure 2: Schematic of crystal structure of Bi₂Se₃. The hexagonal unit cell is comprised of three rhombohedral stacked quintuple layers (QLs). Each of these is terminated by a Se atom, and separated by a van der Waals gap, whereas intra-QL bonding is covalent.

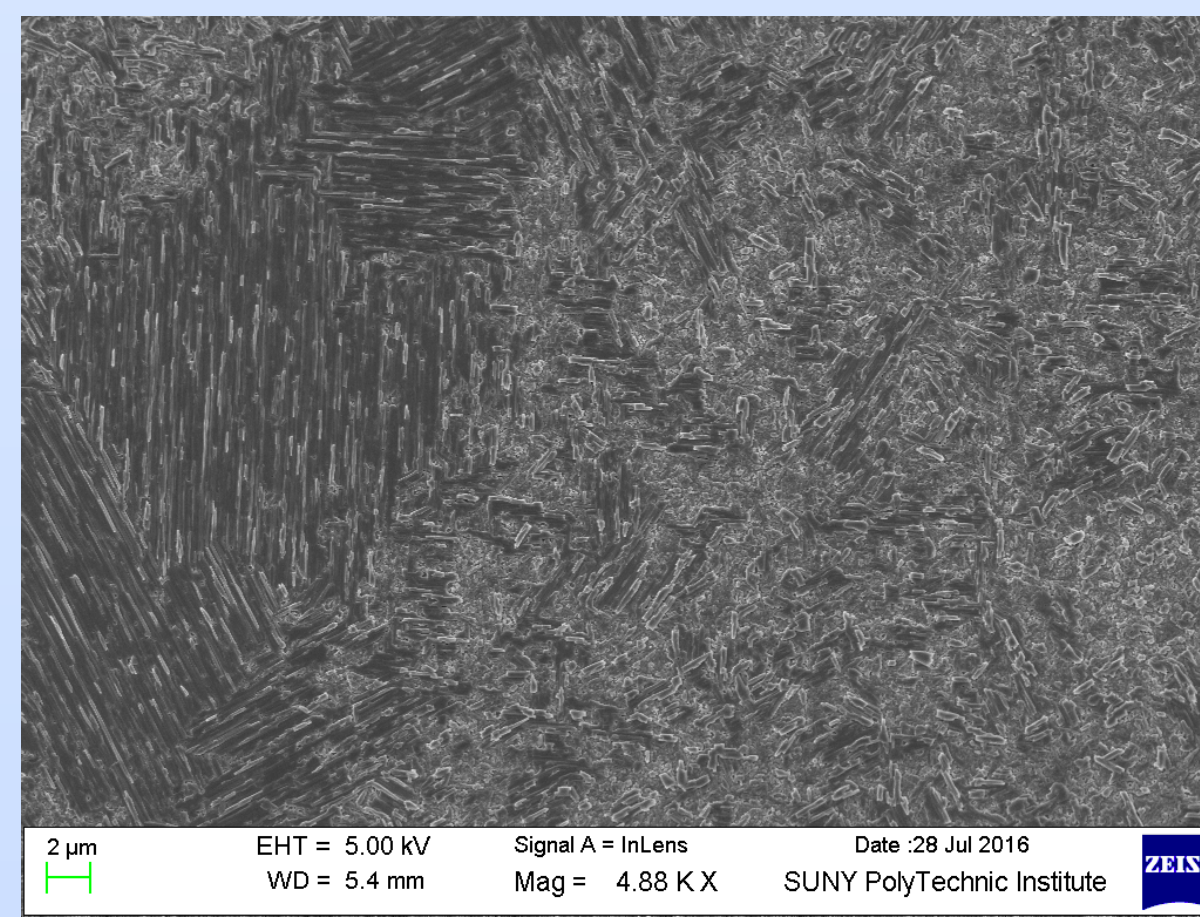


Figure 3: SEM image of the surface of a Se-capped sample. The cap was expected to be amorphous, but crystalline rods are easily visible on the surface. These rods were oriented for areas of up to 50 μm. The thickness of the rods appears nearly equal to the cap height (200 nm). Outside of well aligned areas, the cap is more polycrystalline, but is not amorphous. Because of this polycrystallinity, the cap has high surface roughness.

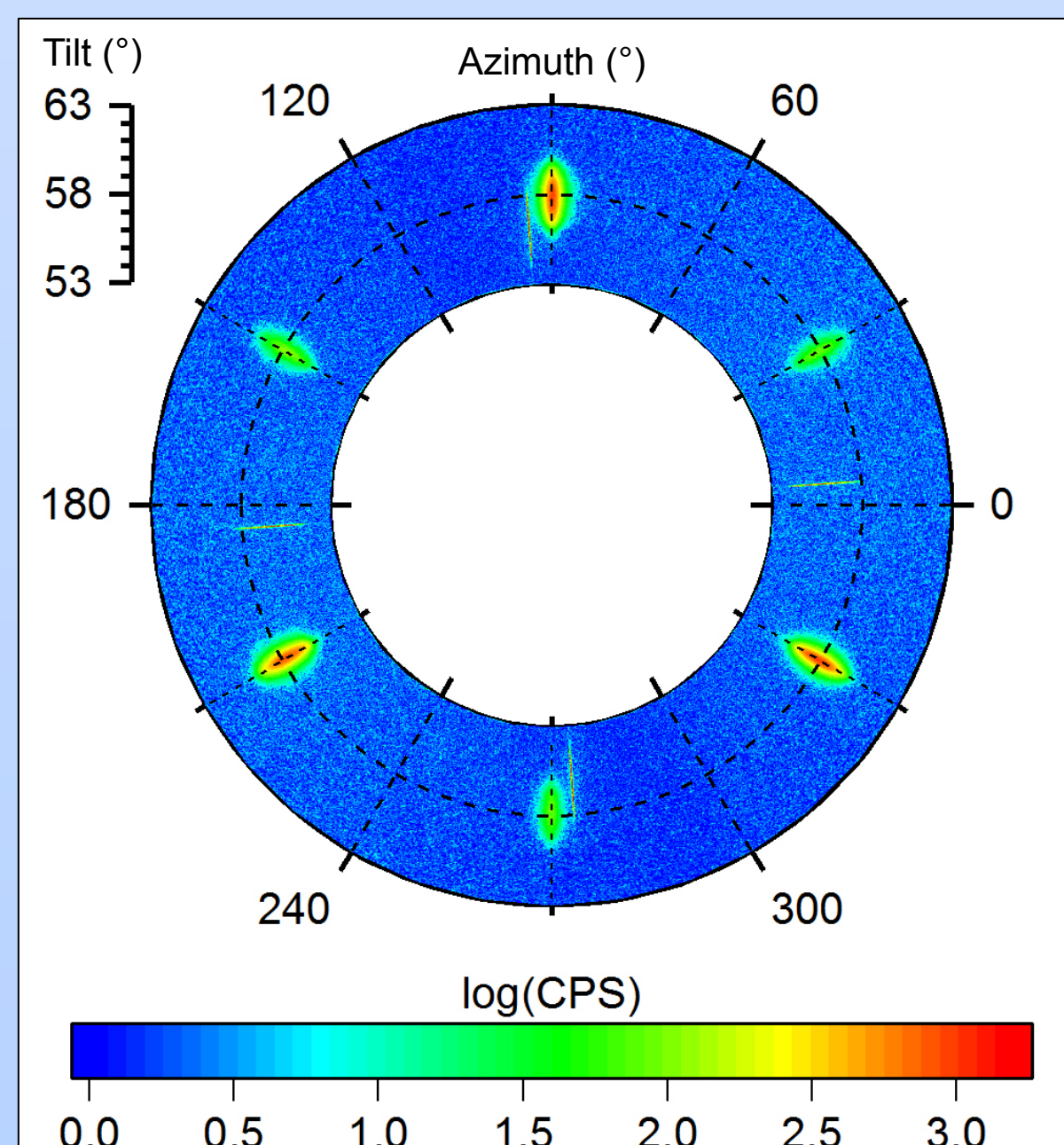


Figure 5: XRD Pole Figure of Bi₂Se₃, measuring the (015) planes. For l=3n, planes are 3-fold symmetric, and grain orientation can be measured. This scan indicates that one grain orientation (along Az = 90 ± 120°) is dominant, which may promote TI performance. 4-fold symmetric (111) streaks are peaks from the Si carrier wafer.

Avery Green¹, Lee Walsh², Wesley Nolting¹, Carl Ventrice¹, Chris Hinkle², and Alain Diebold¹

- College of Nanoscale Science and Engineering, SUNY Polytechnic Institute, 257 Fuller Road, Albany, NY 12203
- Materials Science and Engineering, University of Texas at Dallas, 800 W. Campbell Road, Richardson, TX 75080

Temperature-Programmed Desorption of the Se Cap

Having demonstrated the high crystal quality of these Se-capped Bi₂Se₃ films, the next aim of this study is to generate a repeatable method of removing the Se cap, such that the integrity of the film is maintained for future use in devices. Because the vapor pressure of Se (10⁻⁴ torr near 130 °C) is higher than that of Bi₂Se₃ (shown to be stable above 300 °C), temperature-programmed desorption (TPD) is run between those temperatures.

TPD is a method for observing desorption as a function of temperature in a UHV environment. In our setup, a Se-capped sample was mounted on a Mo plate, and inserted into a UHV chamber. It was then radiatively heated by a W coil, through an aperture in the Mo plate, at a controlled rate. The PC detects the temperature at the surface of the sample with a K-type thermocouple, and adjusts the current through the W coil to maintain the user-defined heating rate (usually 10 °C/min). The mass spectrometer is set to detect ⁷⁸Se, ⁸⁰Se, as well as common contaminants (H₂O, CO₂, CO, and H₂). The heating linearly until a target is reached, hold for 30 minutes, and then cool to room temperature. Target temperatures include 110, 170, 220, 270, 320, and 370 °C.

In samples heated between 130 and 300 °C, there is a sharp desorption spike of Se near 130 °C (Fig. 7). The initial portion of this peak can be modeled with a zero order Polanyi-Wigner equation: $-\frac{d\theta}{dt} = \nu_s e^{-E_a/kT}$, where θ is the coverage and ν_s is a constant. This behavior corresponds to desorption of a bulk material, as is the case with the ~200 nm Se cap. **Until the film is heated to ~300 °C, there is no evidence of desorption coming from the Bi₂Se₃ film. As other characterization methods have not shown significant film degradation, we consider anneals of up to ~300 °C to be safe.** In addition to monitoring the decapping process, TPD provides information about the kinetics of desorption. The zero order Polanyi-Wigner equation gives an Arrhenius relationship for early desorption. **Linear fits to early desorption peak data provides the activation energy of Se, which we calculated to be 1.56 eV (Fig. 8).**

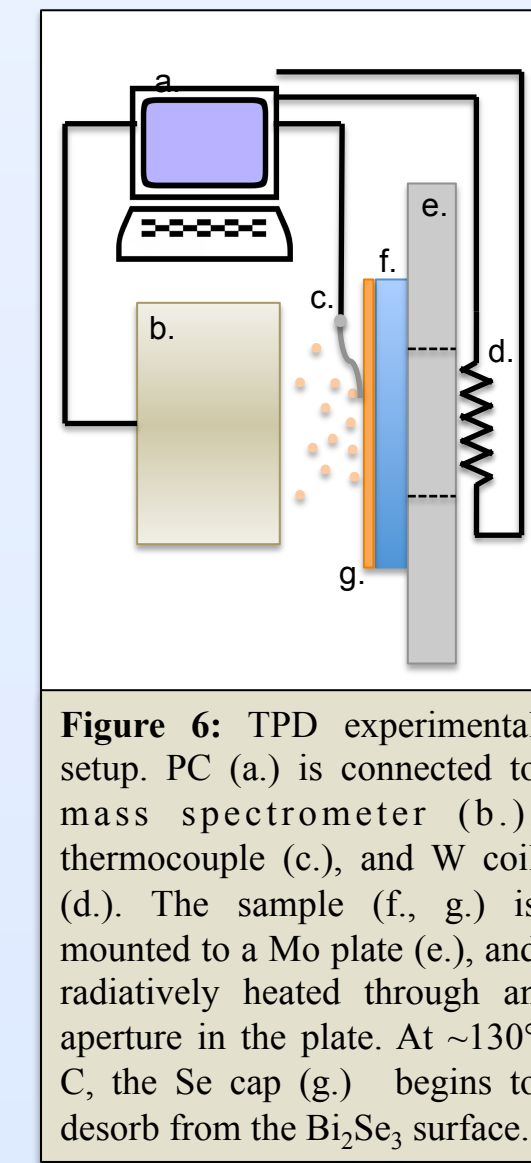


Figure 6: TPD experimental setup. PC (a) is connected to mass spectrometer (b), thermocouple (c), and W coil (d). The sample (e, g) is mounted to a Mo plate (e), and radiatively heated through an aperture in the plate. At ~130 °C, the Se cap (g) begins to desorb from the Bi₂Se₃ surface.

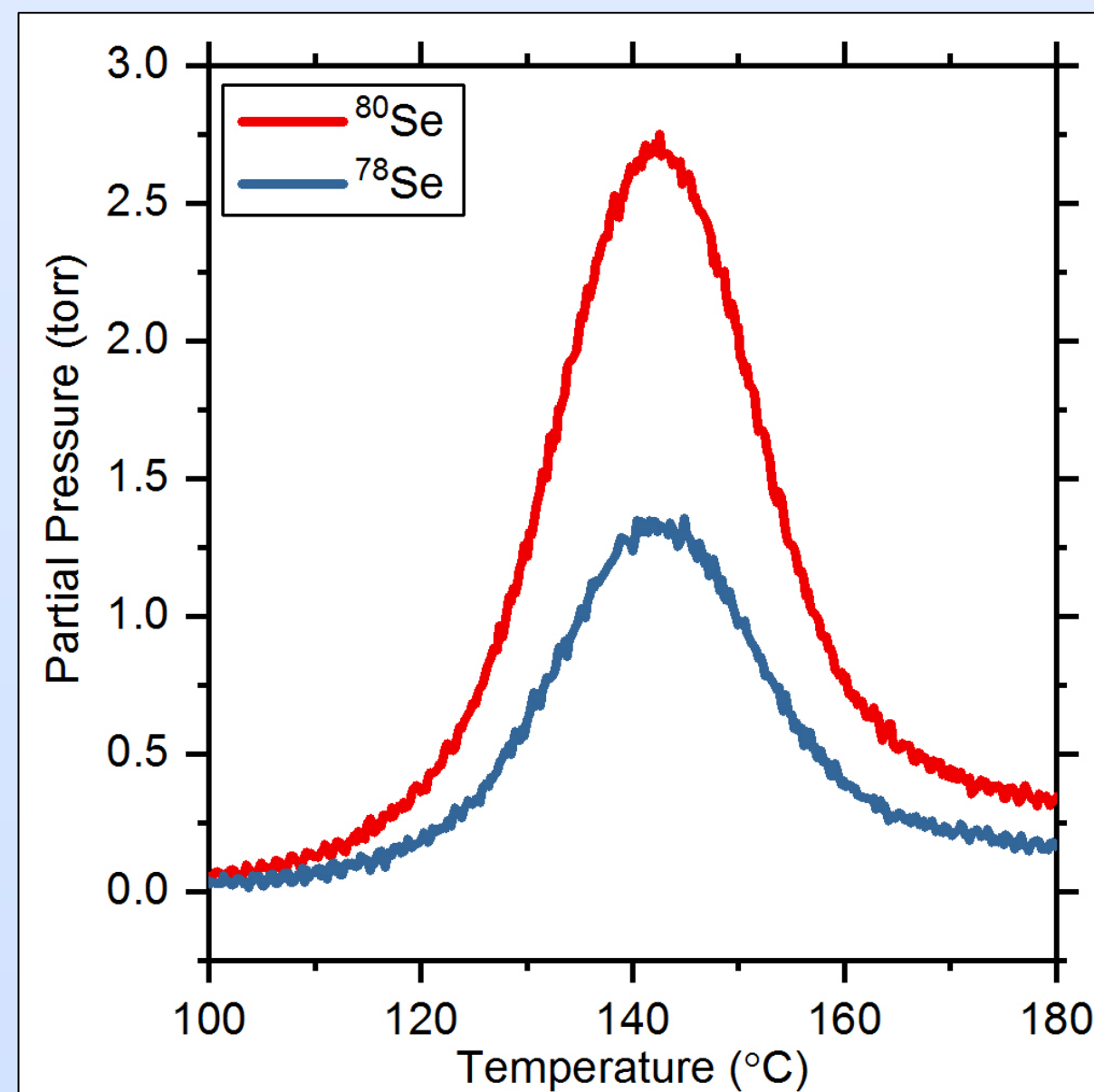


Figure 7: Desorption peak of Se during temperature-programmed desorption (TPD). The expected profile for zero order desorption has a much sharper inflection point at the peak, where a decrease in pressure begins. We explain that this more symmetric desorption behavior is due to the variance in the cap morphology. Its roughness could cause some areas of the film to be exposed before others, thus causing the desorption to exhibit a transition to its first order behavior (where pressure is linearly dependent on remaining coverage).

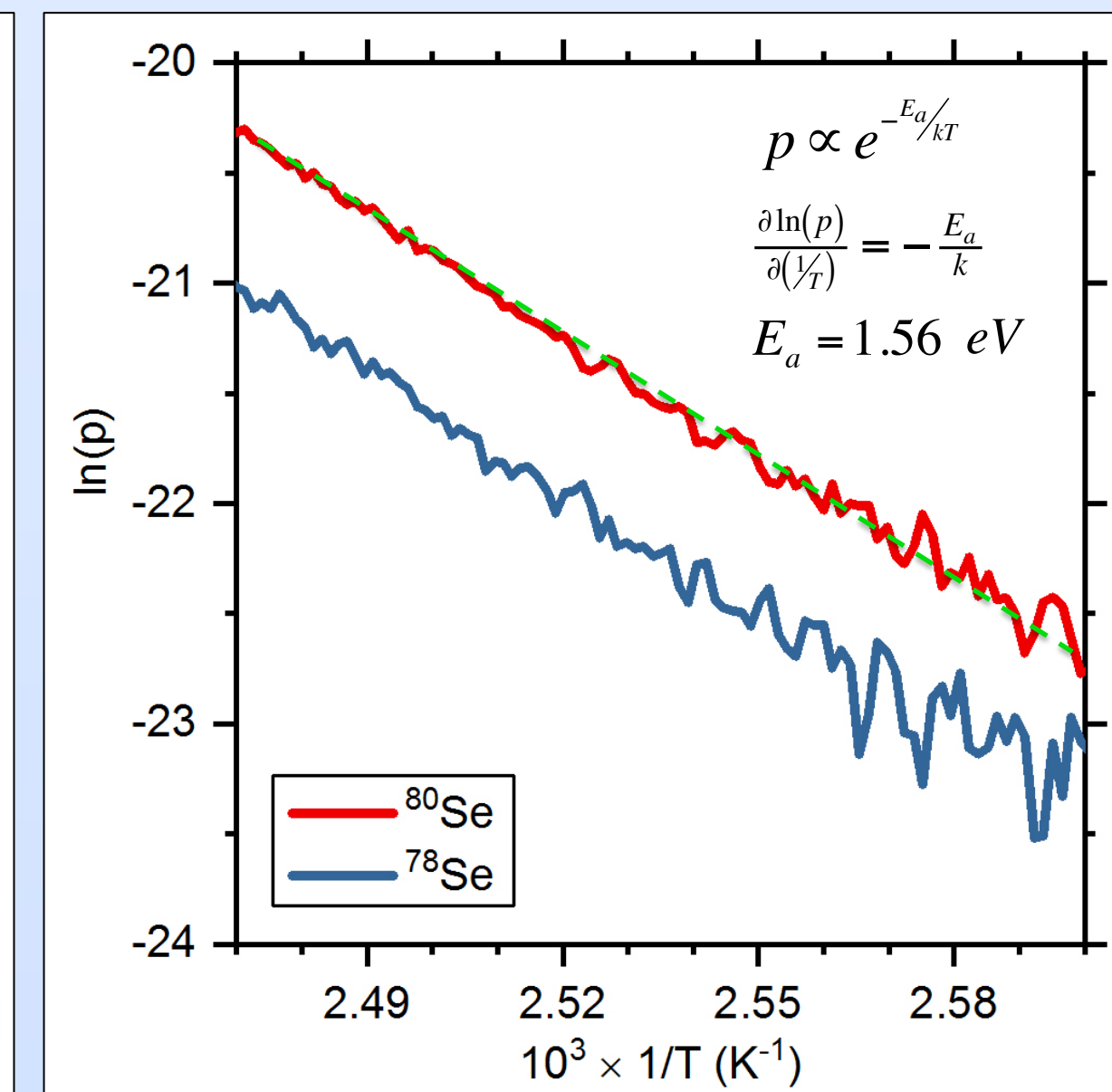


Figure 8: Arrhenius relationship of the zero order section of Se cap desorption peak (111 - 132 °C). With few manipulations, the zero order Polanyi-Wigner equation can provide the activation energy of bulk desorption as a linear slope. Additionally, because ⁸⁰Se and ⁷⁸Se occupy the cap in known proportion (measured to the expected values, 0.496 to 0.238, by peak integration), either can be used to extract the E_a. ⁸⁰Se is chosen for its lower noise value, and E_a = 1.56 eV is calculated.

Post-TPD Bi₂Se₃ Film Surface Morphology

Immediately after TPD, *in situ* LEED is performed on the decapped Bi₂Se₃ films, in order to observe surface crystallinity (Fig. 9). As XRD is a bulk measurement technique, the surface diffraction gathered in this experiment provides complementary information about these samples. However, because the film is thin (~20 nm), it is expected that 'surface' and 'bulk' diffractions should be very similar, with the caveat that LEED truncation rods may contribute to an apparent, but false, 6-fold azimuthal symmetry. **It is found that as in XRD, there are two sets of 3-fold symmetric diffraction spots with slightly differing intensities, which indicates a preferential grain direction.** Subsequently, *ex situ* AFM is performed for direct imaging of the surface grains (Fig. 10). This shows triangular island grain growth for all samples, with grains of up to ~2 μm. **Oppositely oriented triangular grains correspond to the oppositely oriented 3-fold symmetric LEED diffraction points.**

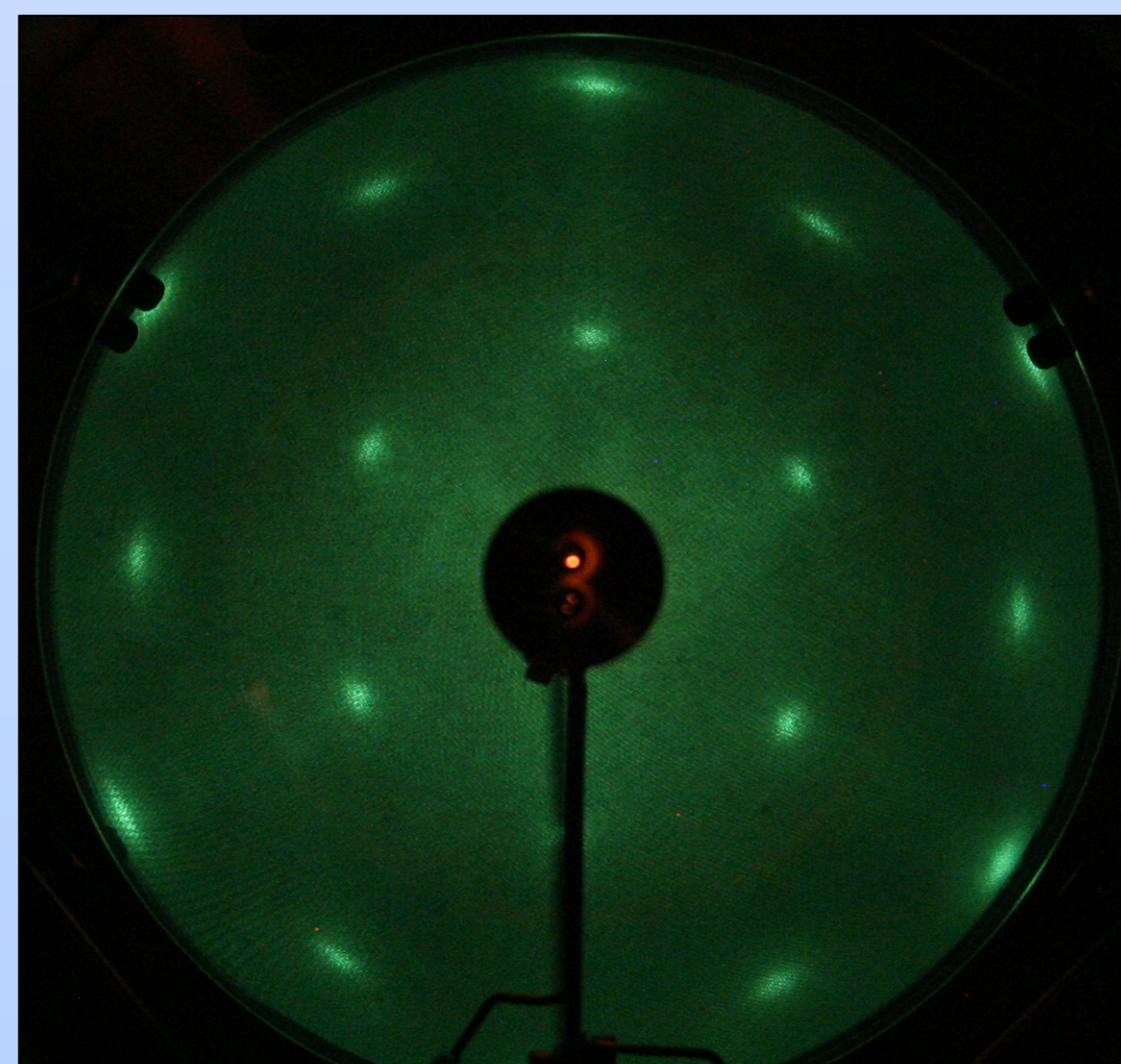


Figure 9: LEED image of a decapped Bi₂Se₃ film surface. With an electron beam energy of 96.3 eV, the Electron mean free path is estimated at 5.4 Å. This resulting in the appearance of HOLZ truncation rod contributions. Diffraction spots at (01l) ± 120° have slightly higher intensity than their complements, indicating a preferred direction among twinned grains.

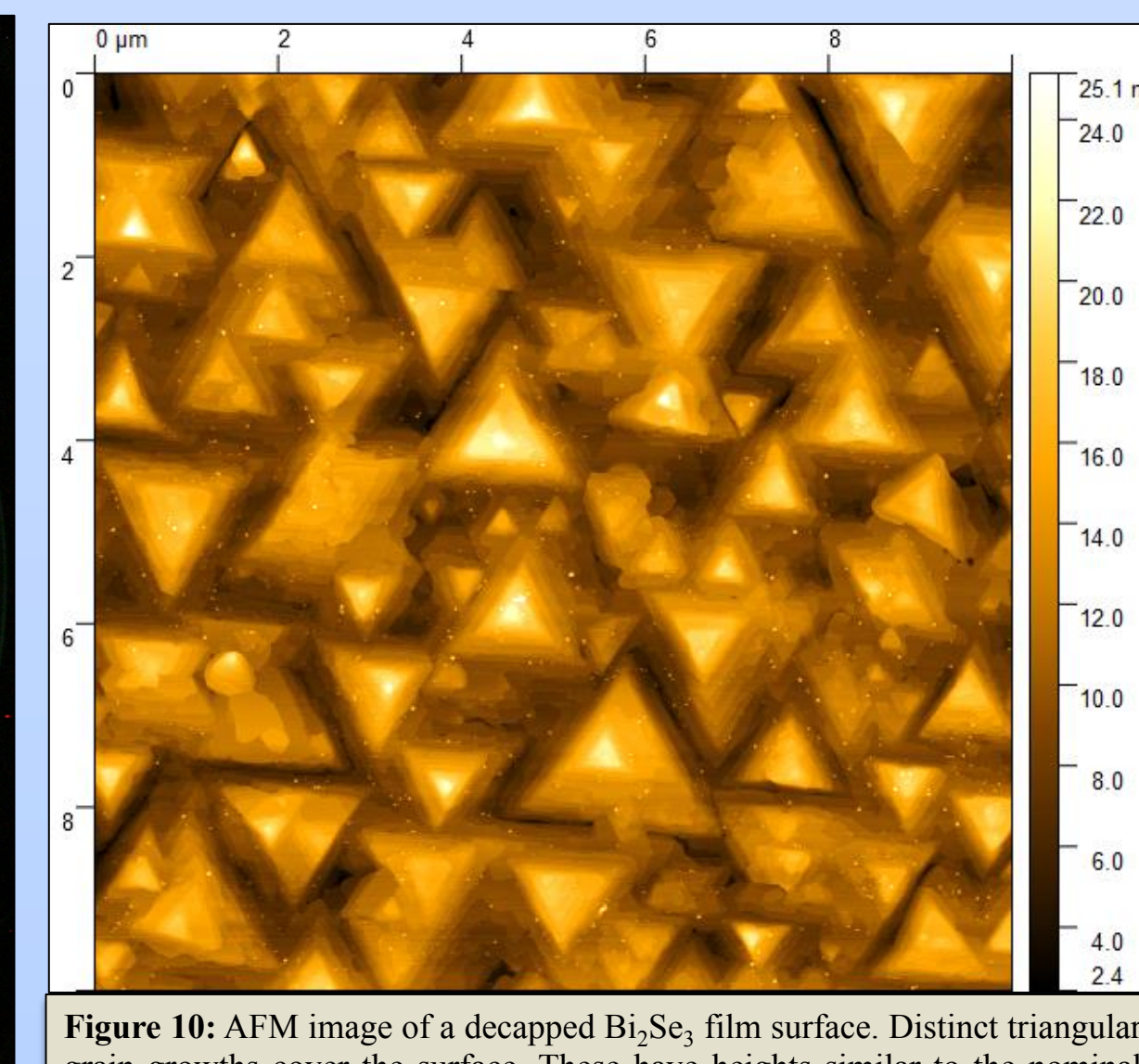


Figure 10: AFM image of a decapped Bi₂Se₃ film surface. Distinct triangular grain growths cover the surface. These have heights similar to the nominal film thickness (20 nm). QL stacking can be seen along triangular edges, showing that TPD anneals cause minimal damage to the film crystallinity. Ordered azimuthal grain orientation is apparent, with opposite island growth directions corresponding to the complementary diffraction points seen in XRD and LEED. This image is from an earlier sample, which had equal diffraction intensities from both 3-fold symmetric point sets.

Characterization of Se Bonding Before and After Decapping

XPS is performed to measure the chemical environment near the surface of capped and decapped Bi₂Se₃ films. Because Se bonds differ between the cap and film (Se-Se bonds exist in the cap, whereas exclusively Se-Bi bonds exist in the film), Se bonding energy may be used to characterize the efficiency of the TPD decapping process. **Se-Se (Fig. 11 a) bonding in the cap creates a higher Se 3d binding energy than Se-Bi (Fig. 11 b) bonding does in the film (ΔE_B = 1.16 eV). We therefore measure this energy after decapping to confirm that no Se is left on the surface, indicating that the film is ready for contact in device applications. We find that for anneals above 130 °C that maintain a target temperature for ≥ 30 min, no Se-Se bonding remains at the surface, and the Se cap is completely desorbed.**

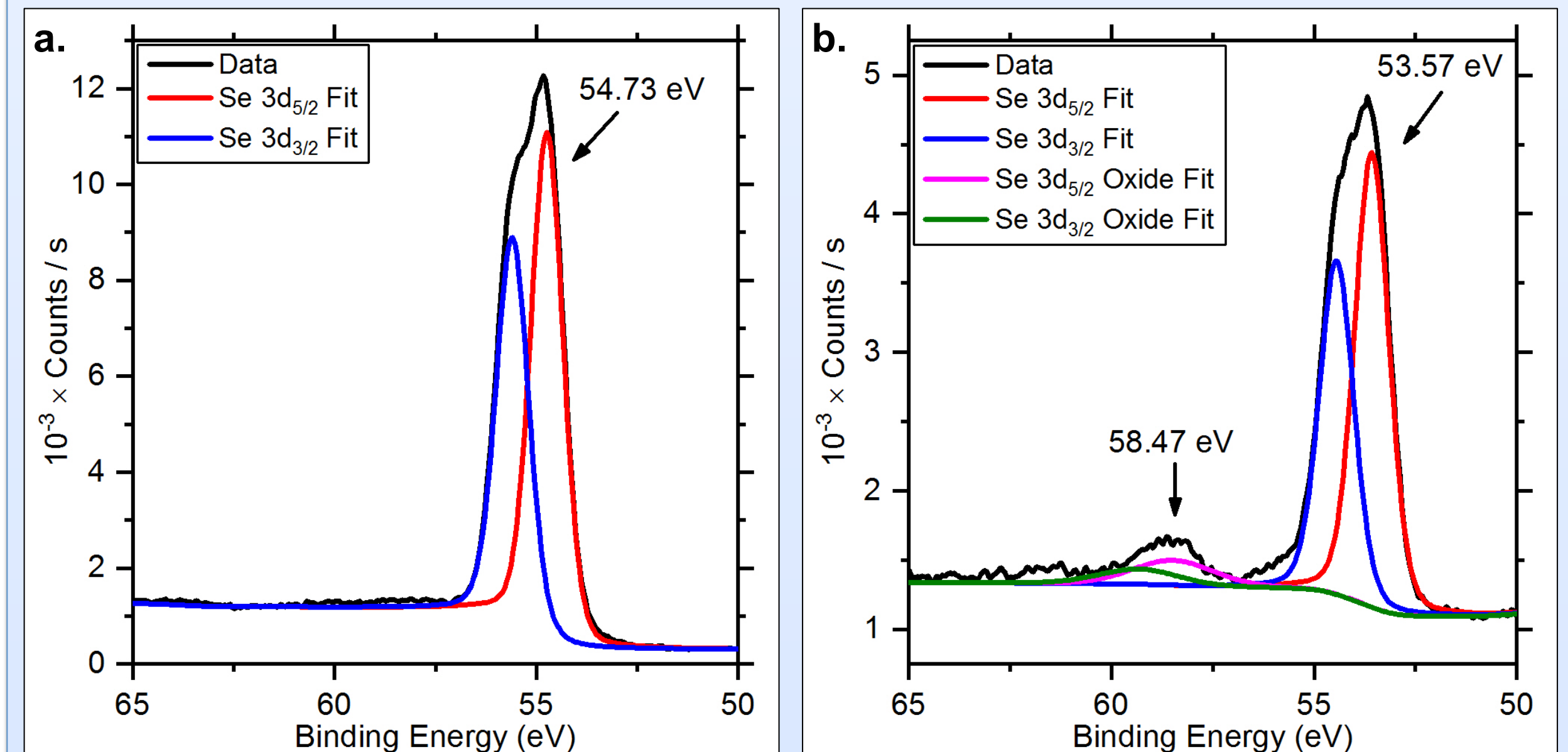


Figure 11: XPS spectrum and fit of Bi₂Se₃ films, before (a.) and after (b.) removing the thick Si cap, at the Se 3d photoelectron energy. There is a 1.16 eV difference in the binding energy of Se 3d electrons for Se atoms with Se-Se and Se-Bi. Bi₂Se₃ contains covalent, octahedral bonds between atoms, such that Bi is bound to Se, and vice versa, and neither Bi-Bi nor Se-Se bonds exist. Because the energy shift is well above the XPS resolution, it can be used to monitor cap desorption, and to qualify if the film is unexposed, partially exposed, or completely exposed. For an anneal of 170 °C, the appears to be no Se-Se bonding remaining at the surface, and thus the film has been completely decapped. Other spectra show strong Bi peaks, but as these do not definitively characterize partial decapping, they are not shown.

Measurement of the Fermi Level at the Surface of Decapped Bi₂Se₃ Films

The final step in this study is to measure the Fermi level at the surface. Many ARPES experiments have shown Dirac cones in Bi₂Se₃ that are shifted to lower energies, often leaving the Fermi level inside the conduction band. Some experiments aimed at reducing this effect have employed Ca or other dopants in order to move E_F into the gap, in anticipation of Se vacancy formation. We show that the Fermi level level can be maintained by capping the samples with Se, and that thermally decapping the samples does not cause the Fermi level to shift into either bulk band. We employ scanning tunneling spectroscopy (STS) to measure the local density of states (LDOS) of the Bi₂Se₃ films. Because the LDOS approaches zero near the Dirac point, this provides a method of measuring the offset between the E_F and the energy at the Dirac point, E_D. After STM imaging, I/V spectra are acquired over many points, and a lock-in amplifier is used to extract dI/dV curves (Fig. 12 a). These are automatically fit after the experiment with a quadratic function in order to remove noise and locate the energy of the minimum LDOS relative to E_F. **We show that Fermi level in the Bi₂Se₃ film is maintained within the band gap after decapping, and that over significant sample areas, remains at 40 ± 5 eV above E_D (Fig. 12 b).**

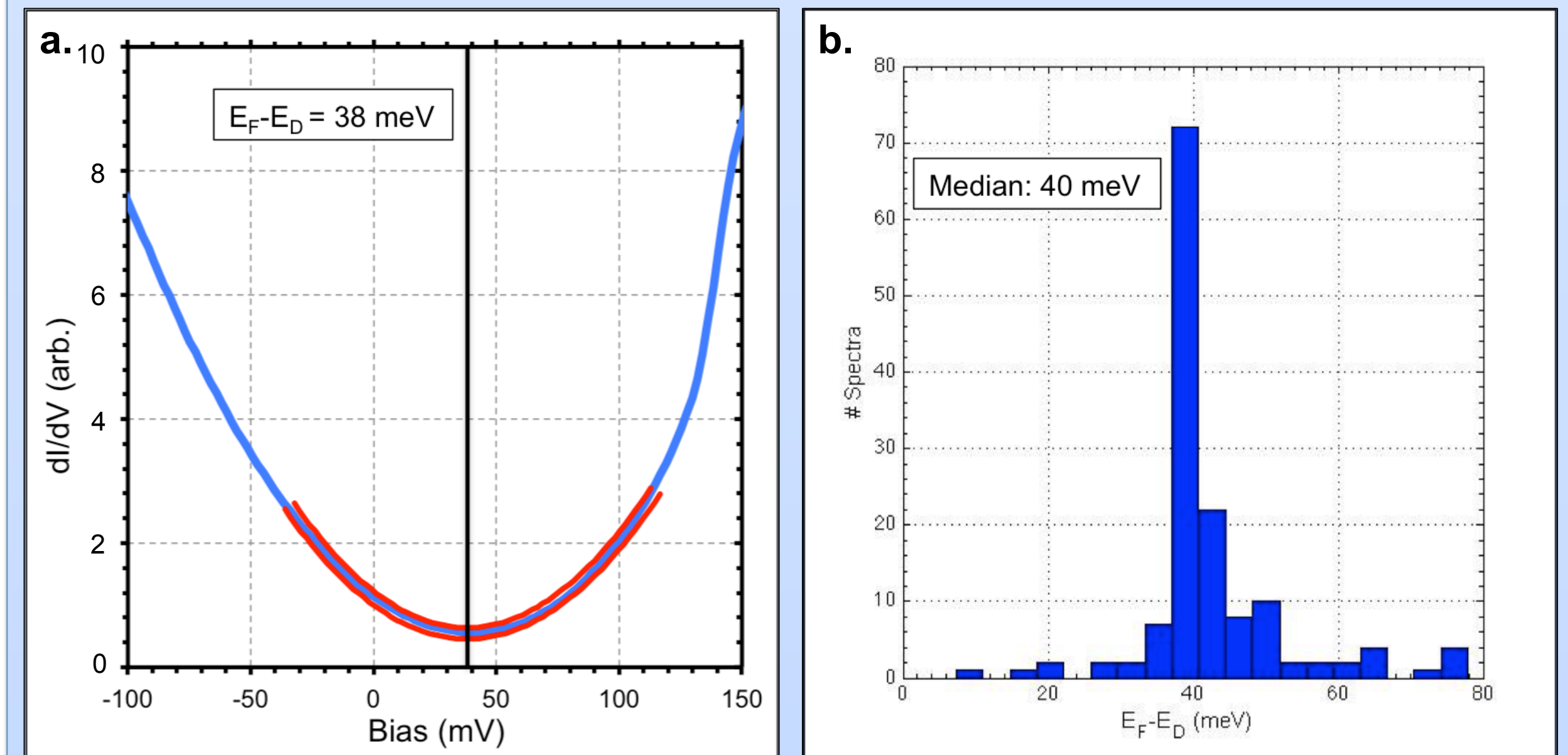


Figure 12: STS dI/dV curve with quadratic fit (a.) and histogram of E_F - E_D over a 1 μm² region (b). These dI/dV spectra are proportional to the electronic local density of states (LDOS) where the data is taken. Each spectrum is fitted with a quadratic curve near the minimum (although near 0 K, a linear LDOS is expected for Dirac cones), and the Fermi level is extracted from the fit. Combining the data taken over a 1 μm² region, a trend of a 40 meV shift of the E_F above the E_D is easily observed. There is some spatial variance, but the majority of the data is in the range 40 ± 5 meV. Because the band gap of Bi₂Se₃ is ~300 meV, this shift leaves the Fermi level inside the band gap, and thus conduction from bulk bands is avoided.

Conclusion and Acknowledgements

In conclusion, we have shown the following:

- MBE growths of Se-capped Bi₂Se₃ thin films on Al₂O₃ substrates are highly crystalline.
 - QLs are vertically stacked on the substrate, lay flat through the film, and contain no measurable Bi bilayers.
 - In recent growths, grain twinning is minimized. Grains are well aligned in a given azimuthal direction.
- Se caps are crystalline with the Bi₂Se₃/Se interface occurring at the (00l)/(h00) planes. The Se cap is also highly polycrystalline and rough.
- The Se cap desorbs when heated above 130 °C. The film appears to remain undamaged for anneal temperatures below 300 °C
- The activation energy of desorption, E_a = 1.56 eV, as calculated with an Arrhenius fit.
- The Bi₂Se₃ surface remains highly crystalline and 3-fold symmetric after annealing, as measured with *in situ* LEED and *ex situ* AFM.
 - Despite some surface twinning, LEED shows a dominant grain surface alignment direction.
- XPS shows that the cap is completely desorbed, up to measurement sensitivity limits, and that Se-Bi bonds dominate XPS signal after decapping.
- The Fermi level is maintained near the Dirac point after capping.
 - STS dI/dV shows DOS minima near a +40 mV bias, indicating a Fermi energy shift of +40 meV above the Dirac point
 - Experimental repetition shows that this E_F - E_D is spatially consistent for a sample heated to ~170 °C.

Thus, we have achieved the goal of decapping a Bi₂Se₃ thin film such that it remains pristine, with surface states that may be used in future devices. We would like to thank the SRC INDEX program for providing funding for this work. The authors at CNSE would also like to thank our co-authors at UT-Dallas for their work in this collaboration. We received additional assistance and guidance from Tyler Mowll, Prof. Vince Labella and Prof. Brad Thiel at CNSE, as well as Prof. Robert Hull of RPI and Prof. Ken Burch of Boston College. Finally, we'd like to thank Dr. George Orji at NIST, who was instrumental in our AFM acquisitions.

